iScience

CellPress
OPEN ACCESS

Article

Apoferritin improves motor deficits in MPTP-treated mice by regulating brain iron metabolism and ferroptosis

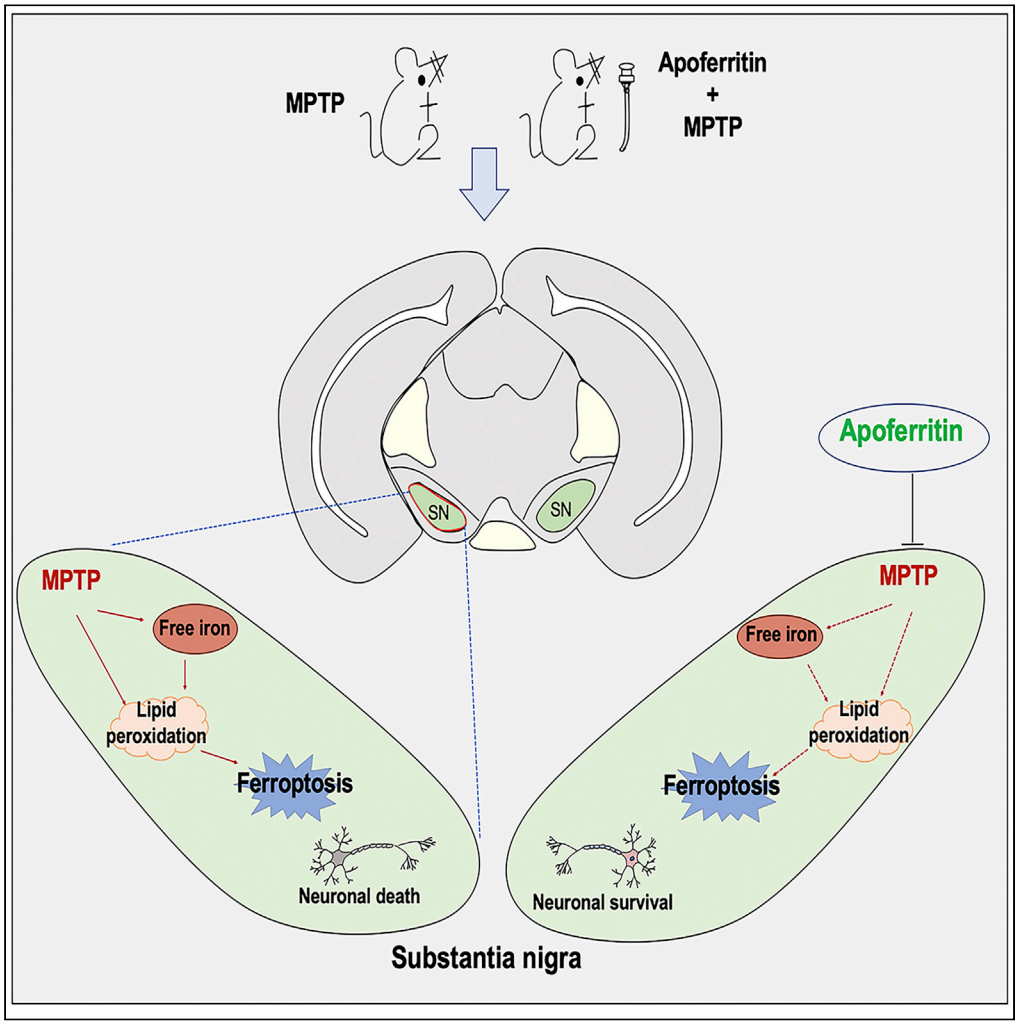

Li-Mei Song, Zhi-Xin Xiao, Na Zhang, Xiao-Qi Yu, Wei Cui, Jun-Xia Xie, Hua-Min Xu

jxiaxie@public.qd.sd.cn (J.-X.X.)
huamin102@163.com (H.-M.X.)

Highlights

Apoferritin improved MPTP-induced motor deficits.

Apoferritin rescued dopaminergic neurodegeneration in the SN of MPTP-treated mice.

Apoferritin inhibited MPTP-induced iron aggregation.

Apoferritin prevented MPTP-induced ferroptosis by regulation of ACSL4 and FSP1.

Song et al., iScience 24, 102431
May 21, 2021
https://doi.org/10.1016/j.isci.2021.102431

iScience

CellPress
OPEN ACCESS

Article

Apoferritin improves motor deficits in MPTP-treated mice by regulating brain iron metabolism and ferroptosis

Li-Mei Song,[1] Zhi-Xin Xiao,[1] Na Zhang,[1,2] Xiao-Qi Yu,[1,2] Wei Cui,[1] Jun-Xia Xie,[2,*] and Hua-Min Xu[1,2,3,*]

SUMMARY

Iron deposition is one of the key factors in the etiology of Parkinson's disease (PD). Iron-free-apoferritin has the ability to store iron by combining with a ferric hydroxide-phosphate compound to form ferritin. In this study, we investigated the role of apoferritin in 1-methyl-4-phenyl-1,2,3,6-tetrahydropyridine (MPTP)-induced PD mice models and elucidated the possible underlying mechanisms. Results showed that apoferritin remarkably improved MPTP-induced motor deficits by rescuing dopaminergic neurodegeneration in the substantia nigra. Apoferritin inhibited MPTP-induced iron aggregation by down-regulating iron importer divalent metal transporter 1 (DMT1). Meanwhile, we also showed that apoferritin prevented MPTP-induced ferroptosis effectively by inhibiting the up-regulation of long-chain acyl-CoA synthetase 4 (ACSL4) and the down-regulation of ferroptosis suppressor protein 1 (FSP1). These results indicate that apoferritin exerts a neuroprotective effect against MPTP by inhibiting iron aggregation and modulating ferroptosis. This provides a promising therapeutic target for the treatment of PD.

INTRODUCTION

Parkinson's disease (PD) is a neurodegenerative disease that is common in middle-aged and elderly people. The pathological feature of PD is the damage of dopamine (DA) neurons in the substantia nigra pars compacta (SNpc), resulting in the progressive loss of motor functions. However, the etiology and pathogenesis are currently not fully understood. Increasing evidence has confirmed that iron content in the substantia nigra (SN) of patients with PD increased significantly compared with the control (Gerlach et al., 2006; Chen et al., 2019; Bergsland et al., 2019; Hirsch, 2009; Dexter et al., 1989; Hopes et al., 2016). Excessive labile iron in the SN resulted in oxidative stress and increased the production of reactive oxygen species (ROS) by the Fenton reaction (Wypijewska et al., 2010; Dixon and Stockwell, 2014; Weinreb et al., 2013). Iron is also an important participant in ferroptosis, which is a newly discovered iron-dependent cell death and has been found in patients with PD (Mahoney-Sánchez et al., 2021; Bellinger et al., 2011; Vallerga et al., 2020). It has also been reported that ferroptosis is related to the pathogenic changes observed in PD models, including elevated iron deposit in the SN, consumption of glutathione (GSH), lipid peroxidation, increased production of ROS, and oxidation of DA (Wypijewska et al., 2010; Dixon et al., 2012). Therefore, it is important to find therapeutic target to prevent iron deposition and iron-dependent ferroptosis in PD.

Studies have confirmed that the cellular mechanism leading to iron accumulation in the SN of PD might be related to abnormal brain iron metabolism (Hentze et al., 2010; Wang and Pantopoulos, 2011; Zecca et al., 2001, 2004). Iron homeostasis is maintained by interactions between iron transporters and iron storage protein. Impaired iron transport or altered iron storage could disrupt the balance of iron homeostasis. Transferrin (Tf)-transferrin receptor (TfR) and the divalent metal transporter 1 (DMT1)-mediated non-transferrin binding iron (NTBI) are two major pathways responsible for iron uptake (Moos and Morgan, 2000; Kielmanowicz et al., 2005). A large number of experiments have confirmed that the up-regulation of iron importer DMT1 might be involved in nigral iron accumulation and the degeneration of DA neurons in PD (Salazar et al., 2008; Saadat et al., 2015; Hirsch, 2009). Iron storage protein ferritin was known to play an important role in maintaining iron homeostasis. Ferritin is composed of 24 subunits of two types: H-ferritin (FTH) and L-ferritin (FTL) (Arosio et al., 1978; Harrison and Arosio, 1996). FTH has ferrous oxidase activity and can oxidize ferrous iron into ferric iron. FTL has a nucleation site to promote the formation of iron core and

[1]Department of Physiology, Shandong Provincial Key Laboratory of Pathogenesis and Prevention of Neurological Disorders, School of Basic Medicine, Qingdao University, Qingdao, 266071, China

[2]Institute of Brain Science and Disease, Qingdao University, Qingdao, China

[3]Lead contact

*Correspondence: jxiaxie@public.qd.sd.cn (J.-X.X.), huamin102@163.com (H.-M.X.)

https://doi.org/10.1016/j.isci.2021.102431

complete iron storage. Evidence has shown that the load of ferritin is significantly increased in PD models (Kaur et al., 2007; Goto et al., 1996). It has been reported that the extracellular ferritin interacts with the cell through the specific binding of FTH to transferrin receptor 1 (TfR1) (Fan et al., 2012; Daniels et al., 2006). The discovery of extracellular ferritin indicated that ferritin might be an important factor in the regulation of brain iron homeostasis.

Apoferritin is an iron-free form of ferritin, which has been used as a non-toxic nanomaterial in clinical treatments such as drug delivery, *in vivo* imaging, and photothermal therapy (Truffi et al., 2016; Srinivasan et al., 2014; Domínguez-Vera et al., 2010). Owing to the iron-binding function, apoferritin might play a role in chelating excess iron to protect DA neurons against PD. In this study, 1-methyl-4-phenyl-1,2,3,6-tetrahydropyridine (MPTP) was used to induce PD mice models. We explored the effects of apoferritin on MPTP-induced motor deficits and elucidated the possible underlying mechanisms. Our results showed that apoferritin could remarkably improve the MPTP-induced motor deficits and inhibit nigral iron aggregation and ferroptosis. This provides new discoveries and possibilities for the prevention and treatment of PD.

RESULTS

Apoferritin pretreatment rescued the weight loss and improved motor deficits induced by MPTP

In this study, we investigated the potential therapeutic effects of apoferritin in MPTP-induced PD mice model. The experimental paradigm is shown in Figure 1A. Results showed that the body weight of MPTP-treated mice decreased significantly compared with the control. And pretreatment with 10 or 15 mg/kg apoferritin had a significant recovery on the weight loss induced by MPTP. There was no difference between the apoferritin group and the control group (Figures 1B and 1C).

Then, we tested the effect of apoferritin on motor ability of MPTP-treated mice using the open-field test and pole-climbing test. Our results showed that MPTP mice exhibited a significantly reduced capacity for pole-climbing, including a significantly longer climb time and longer time to turn their heads. Pretreatment with 10 or 15 mg/kg apoferritin improved the pole-climbing ability (Figures 1D and 1E). There is no significant difference between 10 mg/kg apoferritin and 15 mg/kg apoferritin pretreatment. Therefore, 10 mg/kg apoferritin pretreatment was used in the following experiments. Results of open-field test showed that compared with the healthy control group, the total distance in MPTP-treated mice decreased significantly, whereas the total distance in the mice with apoferritin pretreatment was significantly increased compared with the MPTP group (Figures 1F and 1G).

Apoferritin effectively inhibited MPTP-induced degeneration of DA neurons

To further verify whether apoferritin pretreatment has a neuroprotective effect on DA neurons in the SN of MPTP-induced PD mice, tyrosine hydroxylase (TH) staining and western blots were used to evaluate the survival of DA neurons and the level of TH protein in the SN. As shown in Figures 2A and 2B, TH-positive neurons in the SN of MPTP-treated mice were significantly decreased compared with the healthy control. Conversely, pretreatment with apoferritin could effectively inhibit MPTP-induced loss of TH-positive neurons. Furthermore, we also detected the protein level of TH in the SN of mice in different groups. Results showed that the protein level of TH in the SN of MPTP-treated mice was significantly decreased compared with the control. Consistent with the effect on rescuing the loss of TH-positive neurons caused by MPTP, pretreatment with apoferritin could significantly attenuate the decrease in TH protein level in the SN of MPTP-treated mice (Figure 2C). Thus, these results suggested that apoferritin could protect DA neurons against MPTP neurotoxicity.

Apoferritin decreased the number of Iba-1-positive microglia in the SN of MPTP-induced mice

The expression of Iba-1 is a hallmark of microglia in the CNS. In this study, immunofluorescence was used to stain Iba-1-positive microglia. Results showed that MPTP treatment induced a robust increase in the number of Iba-1-positive microglia in the SN as detected by Iba-1 staining, compared with the control. The number of Iba-1-positive microglia markedly decreased after 10 mg/kg apoferritin pretreatment (Figures 3A and 3B). This suggested that the effect of apoferritin on the number of Iba-1-positive microglia in the SN might also contribute to its neuroprotection against MPTP.

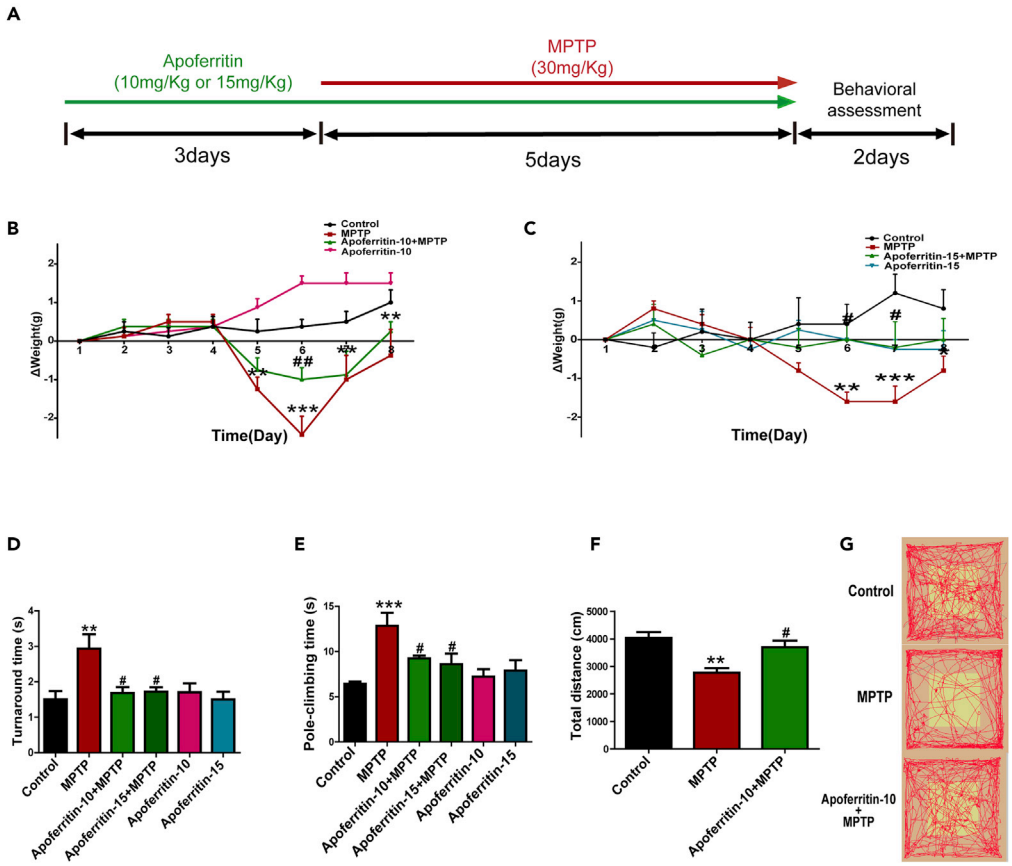

Figure 1. Apoferritin increased the body weight and improved motor deficits of MPTP-induced mice

(A) Experimental scheme of MPTP model.

(B and C) Apoferritin inhibited MPTP-induced weight loss in mice. ΔWeight means the weight change of mice.

(D and E) Injection of MPTP (intraperitoneal) induced a significant increase of pole-climbing time and turnaround time in pole-climbing test, which was inhibited by apoferritin.

(F and G) In the open-field test, the decrease in the total movement distance in 10 min induced by MPTP was also improved by apoferritin.

*$p < 0.05$, **$p < 0.01$, ***$p < 0.001$, compared with the control; $^{\#}p < 0.05$, $^{\#\#}p < 0.01$, compared with the MPTP. Data were expressed as mean ± SEM (n = 5–9 in each group).

Apoferritin decreased iron content in the SN and regulated iron transporters

Increased iron content in the SN of PD has been indicated in patients with PD and PD animal models. Apoferritin is an iron-free ferritin and might exert its neuroprotective effect in PD by chelating excess iron. Therefore, in this study, we investigated the effect of apoferritin on the number of iron-positive cells and the expression of iron transporters in MPTP-induced PD models. Results showed that the number of iron-positive cells in the SN as measured by iron staining was higher in MPTP-treated mice compared with the control. On the contrary, pretreatment with apoferritin suppressed MPTP-induced increase in the number of iron-positive cells in the SN of MPTP-treated mice (Figures 4A and 4B). This indicated that the protection of apoferritin might be related to reducing iron accumulation in the SN of MPTP-induced PD mice.

Consistently, altered expressions of iron-related proteins have been reported to be involved in the nigral iron accumulation in PD. We further investigated whether the effect of apoferritin on iron levels was related to the regulation on the expression of iron-related proteins. Therefore, the expressions of iron importer DMT1 and TfR1 were detected by western blot analysis. Results showed that MPTP-induced PD mice expressed higher levels of DMT1 in the SN than the control mice, and pretreatment with apoferritin drastically inhibited the up-regulation of DMT1 induced by MPTP (Figure 4C). However, the expression of TfR1

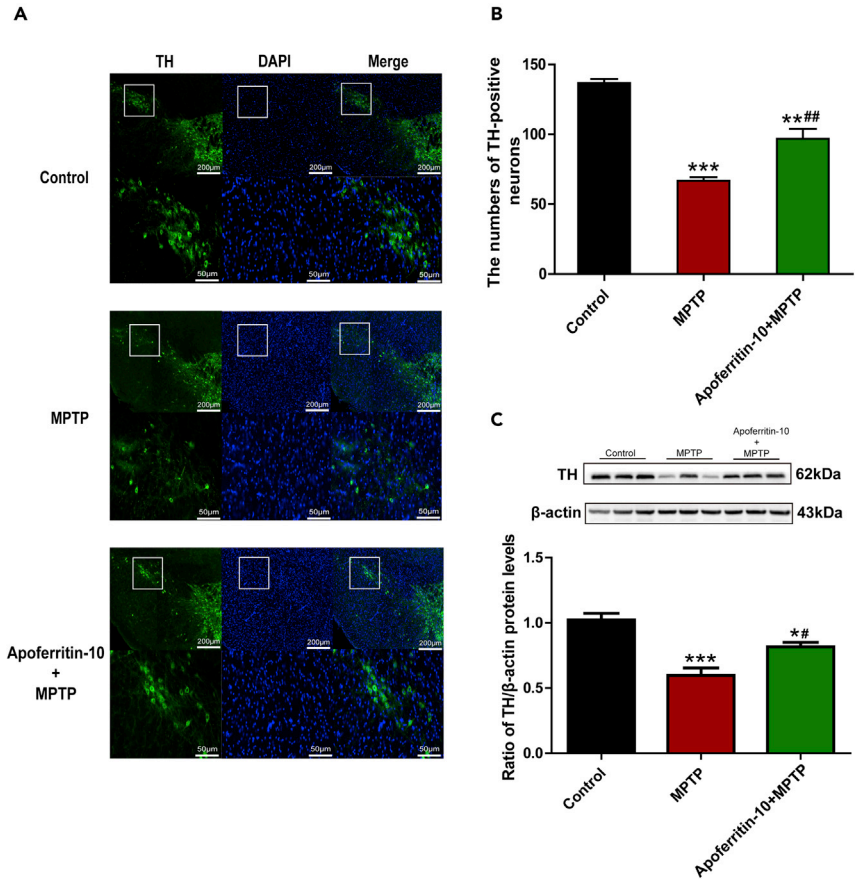

Figure 2. Apoferritin ameliorated MPTP-induced loss of dopaminergic neurons in the SN

(A) The number of TH-positive neurons in the SNpc were significantly reduced after MPTP treatment. Apoferritin ameliorated the loss of TH-positive neurons caused by MPTP. The scale bar represents 200 μm (top) and 50 μm (below).

(B) Statistical analysis of TH-positive neurons as shown in (A).

(C) The expression of TH was reduced in the SN in MPTP-treated mice. Apoferritin suppressed MPTP-induced decrease in the expression of TH. Data were presented as percentage of control.

*$p < 0.05$, **$p < 0.01$, ***$p < 0.001$, compared with the control. $^{\#}p < 0.05$, $^{\#\#}p < 0.01$, compared with the MPTP. Data were expressed as mean ± SEM (n = 8, 9 in each group).

decreased after MPTP treatment, and apoferritin restored the expression of TfR1 in MPTP-treated mice (Figure 4D). Thus, the effect of apoferritin on suppression of nigral iron accumulation in MPTP-induced PD mice might be associated with regulating the abnormal expression of iron import protein DMT1.

Apoferritin protected DA neurons against MPTP by inhibiting ferroptosis

Ferroptosis is an iron-dependent cell death. Studies have confirmed that ferroptosis is involved in the pathology of PD. To further investigate whether apoferritin could inhibit ferroptosis, we conducted the experiments to detect the expressions of proteins related to ferroptosis including glutathione peroxidase 4 (GPX4), long-chain acyl-CoA synthetase 4 (ACSL4), and ferroptosis suppressor protein 1 (FSP1). Results showed that the expression of GPX4 decreased significantly in the SN of MPTP-treated PD mice. However, pretreatment with apoferritin did not restore MPTP-induced decrease in the expression of GPX4 as shown in the Figure 5A. Further study showed that MPTP and pretreatment with apoferritin did not affect the levels of GSH/oxidized glutathione (GSH/GSSG) (Figure 5B). In addition, results showed that the expression of ACSL4 increased, whereas the expression of FSP1 decreased significantly in the SN of MPTP-treated PD mice. Apoferritin pretreatment suppressed MPTP-induced increase in the expression of ACSL4 and decrease in the expression of FSP1 (Figures 5C and 5D). These results indicated that the neuroprotective effect of apoferritin might be associated with the regulation of ferroptosis by affecting the expression of ACSL4 and FSP1.

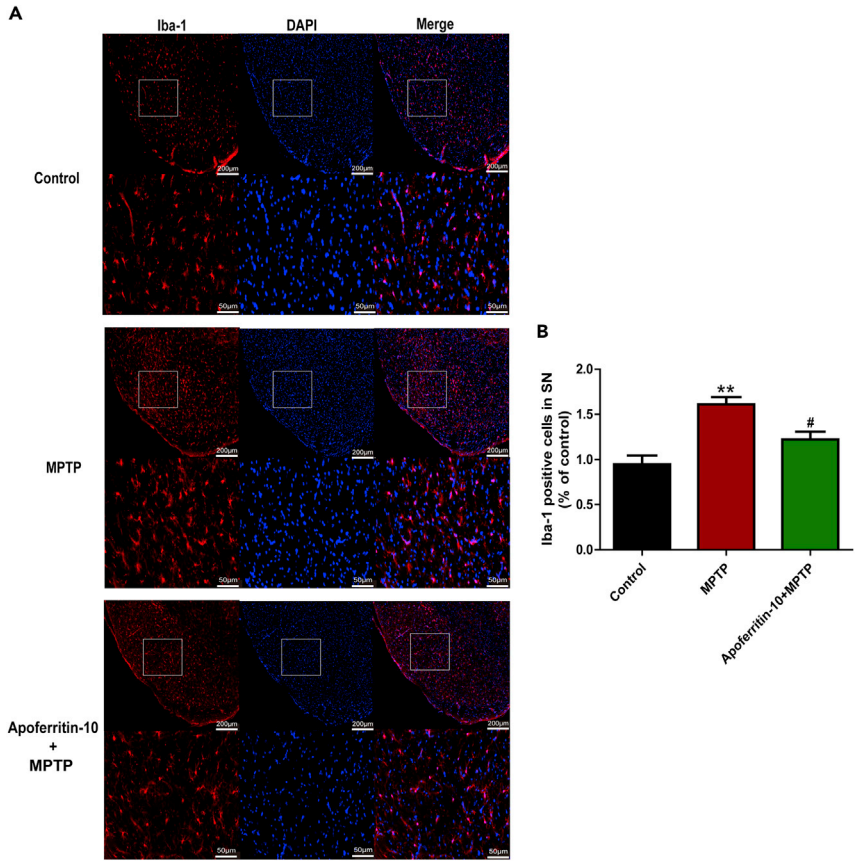

Figure 3. Apoferritin suppressed MPTP-induced increase of Iba1-positive microglia in the SN

(A) MPTP treatment caused a significant increase in the number of Iba1-positive microglia in the SN, which was suppressed by apoferritin. Scale bars, 200 μm (top) and 50 μm (below).

(B) Statistical analysis.

**$p < 0.01$, compared with the control. $^{\#}p < 0.05$, compared with the MPTP. Data were expressed as mean ± SEM (n = 6 in each group).

DISCUSSION

Evidence suggests that iron deposition in the SN is involved in the pathogenesis of PD (Hirsch et al., 1991; Dexter et al., 1987; Riederer et al., 1989). Treatment strategies that inhibit iron accumulation and iron-dependent cell damage might halt the progression of PD. Apoferritin is an iron-free ferritin that has the function of storing iron. Here, we investigated the neuroprotective effect and the possible underlying mechanisms of apoferritin against MPTP toxicity. We presented evidence supporting that apoferritin can effectively improve motor deficits and protect against the degeneration of DA neurons of MPTP-induced PD mice. More importantly, we found that suppression of nigral iron accumulation and regulation of iron transporter DMT1 might contribute to the neuroprotection of apoferritin against MPTP toxicity. Furthermore, we showed here that apoferritin could inhibit MPTP-induced ferroptosis by up-regulating FSP1 and down-regulating ACSL4.

MPTP is a by-product in the synthesis of 1-methyl-4-phenyl-4-propionoxypiperidine (MPPP) (Ziering and Lee, 1947). MPTP itself is not toxic, but after entering the brain, it is converted into toxic 1-methyl-4-phenylpyridiniumion (MPP^+) under the action of monoamine oxidase B. MPP^+ is specifically transported to dopaminergic neurons of the SN by DA transporter and then induces the occurrence of PD by inhibiting mitochondrial complex I (Langston et al., 1984; Chiba et al., 1984; Castagnoli et al., 1985; Lee et al., 2011). Our results demonstrated that apoferritin can prevent MPTP-induced weight loss and improve motor deficits. And there was no significant difference in the protection against MPTP-induced motor deficits between intragastric gavage and intravenous injection of apoferritin (Figure S1). In addition, apoferritin protected against MPTP-induced degeneration of DA neurons, including restoring TH-positive neurons and increasing the expression of TH protein of the SN in MPTP-induced

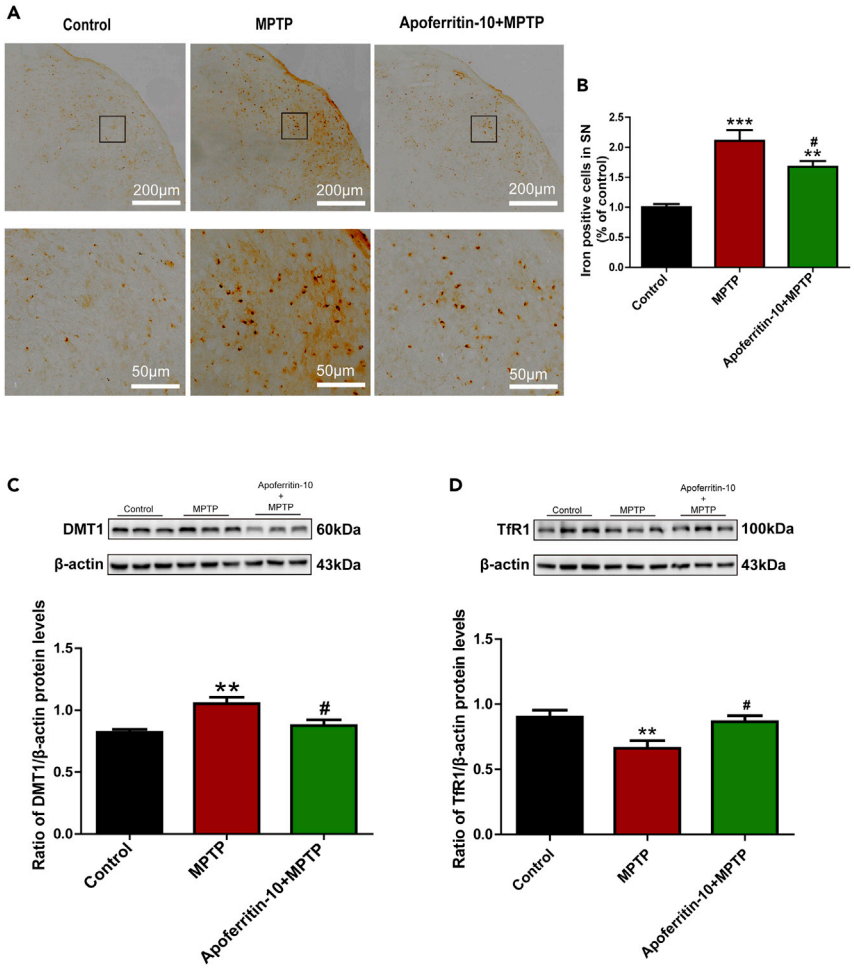

Figure 4. Apoferritin suppressed MPTP-induced iron accumulation in the SN via regulating iron-transport proteins

(A) Perls' iron staining revealed that MPTP treatment resulted in the increase in iron-positive cells in the SN, which could be suppressed by apoferritin. Scale bars, 200 μm (top) and 50 μm (below).

(B) Statistical analysis of iron positive cells as shown in (A).

(C) DMT1 was up-regulated in the SN of MPTP-induced mice. Apoferritin suppressed MPTP-induced up-regulation of DMT1.

(D) The expression of TfR1 decreased in the SN of MPTP-induced mice. Apoferritin suppressed MPTP-induced decrease in the expression of TfR1.

**$p < 0.01$, ***$p < 0.001$, compared with the control. $^{\#}p < 0.05$, compared with the MPTP. Data were expressed as mean ± SEM (n = 5–7 in each group).

PD mice. Further results showed that apoferritin decreased the numbers of Iba-1-positive microglia in the SN of MPTP-induced mice. These results indicate that apoferritin has a protective effect against MPTP-induced neurotoxicity. *In vivo* and *in vitro* results also showed that the expression of L-ferritin in the SN of mice and primary cultured ventral mesencephalon (VM) neurons increased significantly after apoferritin treatment compared with the control. This indicated that apoferritin might exert its effect by entering neurons and capturing intracellular iron (Figure S2).

Studies have confirmed that MPTP induced iron deposition in the SN of mice (Shi et al., 2019; Li et al., 2020; Goto et al., 1996; Temlett et al., 1994). In this study, we also observed the increased iron-positive cells in the SN of MPTP-induced PD mice. And we further proved that apoferritin pretreatment could inhibit MPTP-induced increase of iron-positive cells. DMT1 and TfR1 are two major iron import proteins, responsible for non-transferrin-bound iron import and transferrin-bound iron import, respectively. Our previous study has shown that MPTP induced iron accumulation and up-regulation of DMT1, whereas iron chelator

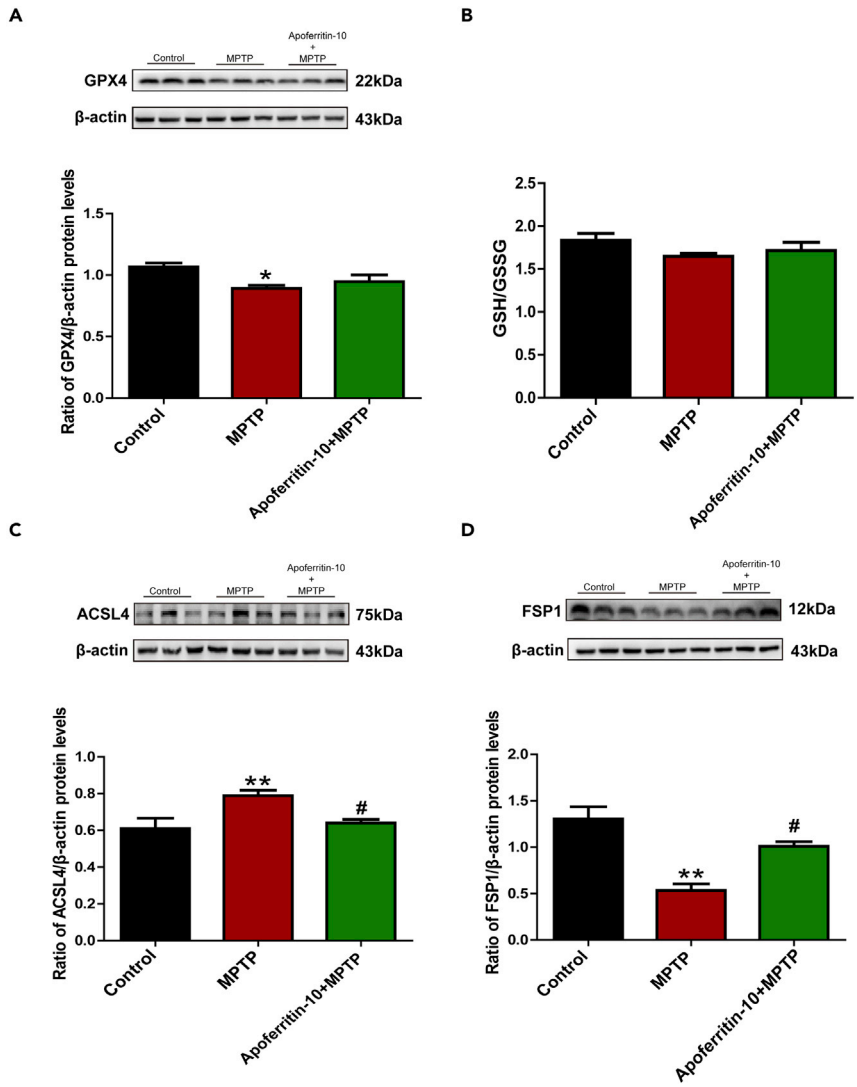

Figure 5. Apoferritin suppressed MPTP-induced ferroptosis in the SN by regulating ferroptosis associated protein

(A) Apoferritin did not restore MPTP-induced decrease in the expression of GPX4.

(B) MPTP and pretreatment with apoferritin did not affect the levels of GSH/GSSG Figures 5C and 5D.

(C) Apoferritin suppressed MPTP-induced up-regulation of ACSL4.

(D) The expression of FSP1 decreased in the SN of MPTP-induced mice, which could be suppressed by apoferritin.

*$p < 0.05$, **$p < 0.01$, compared with the control. $^{\#}p < 0.05$, compared with the MPTP. Data were expressed as mean ± SEM (n = 5–8 in each group).

deferoxamine (DFO) abolished these effects (Zhang et al., 2009). In this study, our results showed that up-regulation of DMT1 in the MPTP-induced PD model was inhibited by apoferritin. This indicated that the iron-suppressing effect of apoferritin might be achieved through the suppression of DMT1, but not TfR1.

Up-regulation of DMT1 might increase iron uptake by neurons, which in turn leads to lipid peroxidation and ROS production by the Fenton reaction (Wypijewska et al., 2010; Aguirre et al., 2012; Dixon and Stockwell, 2014; De Farias et al., 2016). Ferroptosis is an iron-dependent and regulated process of cell death, which is characterized by the accumulation of ROS and lipid peroxidation products. It has been reported that ferroptosis was involved in the neuropathology of MPTP neurotoxicity (Do Van et al., 2016). Previous studies have shown that ferroptosis inhibitors ferrostatin-1 (Fer-1) and liproxstatin-1 can effectively prevent the loss of DA neurons in the SN of PD (Do Van et al., 2016; Dixon et al., 2012), whereas the iron chelator DFO can

effectively inhibit the occurrence of ferroptosis (Cheng et al., 2019). Therefore, apoferritin might protect DA neurons against MPTP by modulating iron homeostasis and iron-dependent ferroptosis.

Glutathione peroxidase 4 (GPX4) is one of the regulator of ferroptosis (Yang et al., 2014) and is essential for maintaining the redox balance of cells (Matsushita et al., 2015). In this study, we investigated the effect of apoferritin on the expression of GPX4 in MPTP-induced PD mice. Results showed that the expression of GPX4 decreased compared with the control. However, apoferritin did not restore MPTP-induced decrease in the expression of GPX4. To further confirm the possible mechanisms underlying the effect of apoferritin on ferroptosis in MPTP-induced PD mice model, we further detected other proteins related to ferroptosis. Recent studies showed that the balance of redox states was regulated by FSP1-NAD (P) H-CoQ10 axis (Bersuker et al., 2019; Doll et al., 2019), which is in parallel with the typical GPX4 pathway to suppress lipid peroxidation and ferroptosis (Doll et al., 2019). As a novel CoQ10 plasma membrane oxidoreductase, FSP1 protects cells from ferroptosis by reduced form of CoQ10, which is a potent antioxidant to prevent lipid peroxidation. Our results showed that MPTP induced decreased FSP1 in the SN, which can be inhibited by apoferritin pretreatment. This indicated that decreased FSP1 might cause CoQ10 to be in an oxidized state and further aggravated lipid peroxidation, leading to the occurrence of ferroptosis and ultimately the degeneration of DA neurons in PD. However, apoferritin can effectively inhibit ferroptosis by up-regulating FSP1, thereby inhibiting the production of lipid peroxidation to exert its neuroprotective effects against MPTP.

In addition, we also detected the expression of ACSL4, a member of the long-chain family of acyl-CoA synthetase proteins, which have recently been shown to play an important role in ferroptosis (Doll et al., 2017). ACSL4 catalyzes arachidonic acid and adrenaline to produce coenzyme A derivatives, which is a process associated with ferroptosis. Free iron or iron-containing lipoxygenase enzymes are responsible for oxidizing membrane polyunsaturated fatty acids (PUFAs), potentially leading to the formation of lipid ROS. It has been reported that ACSL4 was required for the activation or incorporation of PUFAs into membrane phospholipids, which is important in ferroptosis. Inhibiting the expression of ACSL4 prevents lipid peroxidation in ferroptosis and related cell death (Doll et al., 2017). Our results showed that MPTP induced up-regulation of ACSL4, which might aggravate lipid peroxidation, whereas apoferritin can effectively inhibit ferroptosis by inhibiting the expression of ACSL4. The results together with previous studies suggest that ferroptosis is probably an important cell death pathway of DA neurons in MPTP-induced PD mice models, and apoferritin might be a potential drug candidate to pharmacologically modulate the ferroptosis via regulation of ACSL4 and FSP1.

In conclusion, our study demonstrates the effect of apoferritin in MPTP-induced PD animal models and elucidates the possible mechanisms underlying its neuroprotection on DA neurons, which is summarized in Figure 6. Our study supports the pathophysiological significance of ferroptosis in the pathogenic process of MPTP-induced PD animal models. Suppression of iron accumulation and iron-dependent ferroptosis in the brain contributes to the neuroprotection of apoferritin against MPTP. This provides a promising therapeutic direction for the clinical prevention and treatment of PD.

Limitations of the study

The mechanisms underlying the effect of apoferritin on MPTP-induced ferroptosis still need to be elucidated. In addition, the transport of apoferritin in the brain is not experimentally demonstrated.

Resource availability

Lead contact

Further information and requests for resources and reagents should be directed to and will be fulfilled by the lead contact, Hua-Min Xu (huamin102@163.com).

Materials availability

This study did not generate new unique reagents.

Data and code availability

Raw data will be shared upon receipt of a reasonable request.

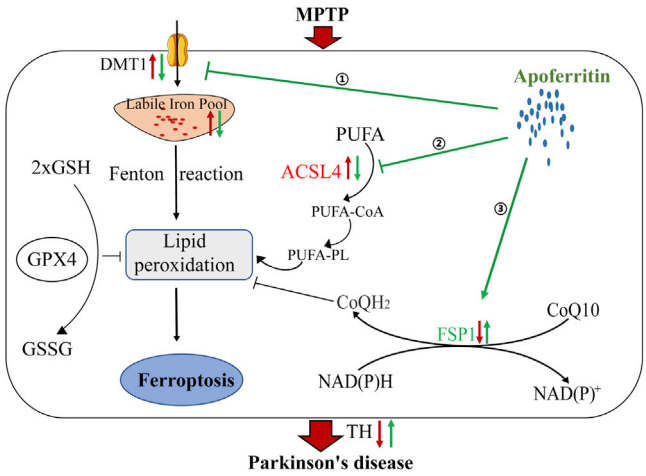

Figure 6. A model of the possible mechanisms underlying the neuroprotective effect of apoferritin against MPTP

MPTP might result in the degeneration of DA neurons through the following pathways: (1) The increase of DMT1 in the SN leads to an increase in iron uptake, which increased the production of ROS by the Fenton reaction, resulting in lipid peroxidation. (2) The increased expression of ACSL4 protein in the SN results in the activation of PUFA, which further aggravates lipid peroxidation. (3) The decreased expression of FSP1 in the SN results in a decrease in the regeneration of reduced CoQ10, which traps lipid peroxidation free radicals, thus leading to ferroptosis. The effect of apoferritin is to abolish the increase in DMT1 and ACSL4 induced by MPTP, and to up-regulate the expression of FSP1 to inhibit lipid peroxidation and ferroptosis. The red arrow represents the changes induced by MPTP, and the blue arrow represents the effect of apoferritin pretreatment.

METHODS

All methods can be found in the accompanying transparent Methods supplemental file.

SUPPLEMENTAL INFORMATION

Supplemental information can be found online at https://doi.org/10.1016/j.isci.2021.102431.

ACKNOWLEDGMENTS

This work was supported by grants from the National Natural Science Foundation of China (31871202, 31771124), the Department of Science and Technology of Shandong Province (ZR2019MC057), Excellent Innovative Team of Shandong Province (2020KJK007), and Taishan Scholars Construction Project, Shandong.

AUTHOR CONTRIBUTION

H.-M.X. conceived the project, designed the experiments, and supervised the project. L.-M.S., Z.-X.X., N.Z., X.-Q.Y., and W.C. performed the experiments. L.-M.S. analyzed the data, prepared the figures, and wrote the manuscript. J.-X.X. revised the manuscript. All authors read and approved the final manuscript.

DECLARATION OF INTERESTS

The authors declare no competing interests.

Received: January 23, 2021
Revised: March 7, 2021
Accepted: April 12, 2021
Published: May 21, 2021

REFERENCES

Aguirre, P., Urrutia, P., Tapia, V., Villa, M., Paris, I., Segura-Aguilar, J., and Núñez, M.T. (2012). The dopamine metabolite aminochrome inhibits mitochondrial complex I and modifies the expression of iron transporters DMT1 and FPN1. Biometals *25*, 795–803.

Arosio, P., Adelman, T.G., and Drysdale, J.W. (1978). On ferritin heterogeneity. Further evidence for heteropolymers. J. Biol. Chem. *253*, 4451–4458.

Bellinger, F.P., Bellinger, M.T., Seale, L.A., Takemoto, A.S., Raman, A.V., Miki, T., Manning-

Boğ, A.B., Berry, M.J., White, L.R., and Ross, G.W. (2011). Glutathione peroxidase 4 is associated with neuromelanin in substantia nigra and dystrophic axons in putamen of Parkinson's brain. Mol. Neurodegener. *6*, 8.

Bergsland, N., Zivadinov, R., Schweser, F., Hagemeier, J., Lichter, D., and Guttuso, T., Jr. (2019). Ventral posterior substantia nigra iron increases over 3 years in Parkinson's disease. Mov Disord. *34*, 1006–1013.

Bersuker, K., Hendricks, J.M., Li, Z., Magtanong, L., Ford, B., Tang, P.H., Roberts, M.A., Tong, B., Maimone, T.J., Zoncu, R., et al. (2019). The CoQ oxidoreductase FSP1 acts parallel to GPX4 to inhibit ferroptosis. Nature *575*, 688–692.

Castagnoli, N., Jr., Chiba, K., and Trevor, A.J. (1985). Potential bioactivation pathways for the neurotoxin 1-methyl-4-phenyl-1,2,3,6-tetrahydropyridine (MPTP). Life Sci. *36*, 225–230.

Chen, Q., Chen, Y., Zhang, Y., Wang, F., Yu, H., Zhang, C., Jiang, Z., and Luo, W. (2019). Iron deposition in Parkinson's disease by quantitative susceptibility mapping. BMC Neurosci. *20*, 23.

Cheng, L.T., Li, Z., Ren, J.J., Niu, Q., Yu, H.M., and Liang, R.F. (2019). [The role of DFO in Al (mal) (3)-induced ferroptosis in PC12 cells]. Zhonghua Lao Dong Wei Sheng Zhi Ye Bing Za Zhi *37*, 722–727.

Chiba, K., Trevor, A., and Castagnoli, N., Jr. (1984). Metabolism of the neurotoxic tertiary amine, MPTP, by brain monoamine oxidase. Biochem. Biophys. Res. Commun. *120*, 574–578.

Daniels, T.R., Delgado, T., Rodriguez, J.A., Helguera, G., and Penichet, M.L. (2006). The transferrin receptor part I: biology and targeting with cytotoxic antibodies for the treatment of cancer. Clin. Immunol. *121*, 144–158.

De Farias, C.C., Maes, M., Bonifácio, K.L., Bortolasci, C.C., De Souza Nogueira, A., Brinholi, F.F., Matsumoto, A.K., Do Nascimento, M.A., De Melo, L.B., Nixdorf, S.L., et al. (2016). Highly specific changes in antioxidant levels and lipid peroxidation in Parkinson's disease and its progression: disease and staging biomarkers and new drug targets. Neurosci. Lett. *617*, 66–71.

Dexter, D.T., Wells, F.R., Agid, F., Agid, Y., Lees, A.J., Jenner, P., and Marsden, C.D. (1987). Increased nigral iron content in postmortem parkinsonian brain. Lancet *2*, 1219–1220.

Dexter, D.T., Wells, F.R., Lees, A.J., Agid, F., Agid, Y., Jenner, P., and Marsden, C.D. (1989). Increased nigral iron content and alterations in other metal ions occurring in brain in Parkinson's disease. J. Neurochem. *52*, 1830–1836.

Dixon, S.J., Lemberg, K.M., Lamprecht, M.R., Skouta, R., Zaitsev, E.M., Gleason, C.E., Patel, D.N., Bauer, A.J., Cantley, A.M., Yang, W.S., et al. (2012). Ferroptosis: an iron-dependent form of nonapoptotic cell death. Cell *149*, 1060–1072.

Dixon, S.J., and Stockwell, B.R. (2014). The role of iron and reactive oxygen species in cell death. Nat. Chem. Biol. *10*, 9–17.

Do Van, B., Gouel, F., Jonneaux, A., Timmerman, K., Gelé, P., Pétrault, M., Bastide, M., Laloux, C., Moreau, C., Bordet, R., et al. (2016). Ferroptosis, a newly characterized form of cell death in Parkinson's disease that is regulated by PKC. Neurobiol. Dis. *94*, 169–178.

Doll, S., Freitas, F.P., Shah, R., Aldrovandi, M., Da Silva, M.C., Ingold, I., Goya Grocin, A., Xavier Da Silva, T.N., Panzilius, E., Scheel, C.H., et al. (2019). FSP1 is a glutathione-independent ferroptosis suppressor. Nature *575*, 693–698.

Doll, S., Proneth, B., Tyurina, Y.Y., Panzilius, E., Kobayashi, S., Ingold, I., Irmler, M., Beckers, J., Aichler, M., Walch, A., et al. (2017). ACSL4 dictates ferroptosis sensitivity by shaping cellular lipid composition. Nat. Chem. Biol. *13*, 91–98.

Domínguez-Vera, J.M., Fernández, B., and Gálvez, N. (2010). Native and synthetic ferritins for nanobiomedical applications: recent advances and new perspectives. Future Med. Chem. *2*, 609–618.

Fan, K., Cao, C., Pan, Y., Lu, D., Yang, D., Feng, J., Song, L., Liang, M., and Yan, X. (2012). Magnetoferritin nanoparticles for targeting and visualizing tumour tissues. Nat. Nanotechnol. *7*, 459–464.

Gerlach, M., Double, K.L., Youdim, M.B., and Riederer, P. (2006). Potential sources of increased iron in the substantia nigra of parkinsonian patients. J. Neural Transm. Suppl. 133–142.

Goto, K., Mochizuki, H., Imai, H., Akiyama, H., and Mizuno, Y. (1996). An immuno-histochemical study of ferritin in 1-methyl-4-phenyl-1,2,3,6-tetrahydropyridine (MPTP)-induced hemiparkinsonian monkeys. Brain Res. *724*, 125–128.

Harrison, P.M., and Arosio, P. (1996). The ferritins: molecular properties, iron storage function and cellular regulation. Biochim. Biophys. Acta *1275*, 161–203.

Hentze, M.W., Muckenthaler, M.U., Galy, B., and Camaschella, C. (2010). Two to tango: regulation of Mammalian iron metabolism. Cell *142*, 24–38.

Hirsch, E.C. (2009). Iron transport in Parkinson's disease. Parkinsonism Relat. Disord. *15* (*Suppl 3*), S209–S211.

Hirsch, E.C., Brandel, J.P., Galle, P., Javoy-Agid, F., and Agid, Y. (1991). Iron and aluminum increase in the substantia nigra of patients with Parkinson's disease: an X-ray microanalysis. J. Neurochem. *56*, 446–451.

Hopes, L., Grolez, G., Moreau, C., Lopes, R., Ryckewaert, G., Carrière, N., Auger, F., Laloux, C., Petrault, M., Devedjian, J.C., et al. (2016). Magnetic resonance imaging features of the nigrostriatal system: biomarkers of Parkinson's disease stages? PLoS One *11*, e0147947.

Kaur, D., Rajagopalan, S., Chinta, S., Kumar, J., Di Monte, D., Cherny, R.A., and Andersen, J.K. (2007). Chronic ferritin expression within murine dopaminergic midbrain neurons results in a progressive age-related neurodegeneration. Brain Res. *1140*, 188–194.

Kielmanowicz, M.G., Laham, N., Coligan, J.E., Lemonnier, F., and Ehrlich, R. (2005). Mouse HFE inhibits Tf-uptake and iron accumulation but induces non-transferrin bound iron (NTBI)-uptake in transformed mouse fibroblasts. J. Cell. Physiol. *202*, 105–114.

Langston, J.W., Irwin, I., Langston, E.B., and Forno, L.S. (1984). 1-Methyl-4-phenylpyridinium ion (MPP+): identification of a metabolite of MPTP, a toxin selective to the substantia nigra. Neurosci. Lett. *48*, 87–92.

Lee, D.H., Kim, C.S., and Lee, Y.J. (2011). Astaxanthin protects against MPTP/MPP+-induced mitochondrial dysfunction and ROS production in vivo and in vitro. Food Chem. Toxicol. *49*, 271–280.

Li, S.J., Ren, Y.D., Li, J., Cao, B., Ma, C., Qin, S.S., and Li, X.R. (2020). The role of iron in Parkinson's disease monkeys assessed by susceptibility weighted imaging and inductively coupled plasma mass spectrometry. Life Sci. *240*, 117091.

Mahoney-Sánchez, L., Bouchaoui, H., Ayton, S., Devos, D., Duce, J.A., and Devedjian, J.C. (2021). Ferroptosis and its potential role in the physiopathology of Parkinson's Disease. Prog. Neurobiol. *196*, 101890.

Matsushita, M., Freigang, S., Schneider, C., Conrad, M., Bornkamm, G.W., and Kopf, M. (2015). T cell lipid peroxidation induces ferroptosis and prevents immunity to infection. J. Exp. Med. *212*, 555–568.

Moos, T., and Morgan, E.H. (2000). Transferrin and transferrin receptor function in brain barrier systems. Cell. Mol. Neurobiol. *20*, 77–95.

Riederer, P., Sofic, E., Rausch, W.D., Schmidt, B., Reynolds, G.P., Jellinger, K., and Youdim, M.B. (1989). Transition metals, ferritin, glutathione, and ascorbic acid in parkinsonian brains. J. Neurochem. *52*, 515–520.

Saadat, S.M., Değirmenci, İ., Özkan, S., Saydam, F., Özdemir Köroğlu, Z., Çolak, E., and Güneş, H.V. (2015). Is the 1254T>C polymorphism in the DMT1 gene associated with Parkinson's disease? Neurosci. Lett. *594*, 51–54.

Salazar, J., Mena, N., Hunot, S., Prigent, A., Alvarez-Fischer, D., Arredondo, M., Duyckaerts, C., Sazdovitch, V., Zhao, L., Garrick, L.M., et al. (2008). Divalent metal transporter 1 (DMT1) contributes to neurodegeneration in animal models of Parkinson's disease. Proc. Natl. Acad. Sci. U S A *105*, 18578–18583.

Shi, L., Huang, C., Luo, Q., Rogers, E., Xia, Y., Liu, W., Ma, W., Zeng, W., Gong, L., Fang, J., et al. (2019). The association of iron and the pathologies of Parkinson's diseases in MPTP/MPP(+)-Induced neuronal degeneration in non-human primates and in cell culture. Front. Aging Neurosci. *11*, 215.

Srinivasan, A., Rastogi, A., Ayyavoo, V., and Srivastava, S. (2014). Nanotechnology-based approaches for the development of diagnostics, therapeutics, and vaccines. Monoclon. Antib. Immunodiagn. Immunother. *33*, 186–191.

Temlett, J.A., Landsberg, J.P., Watt, F., and Grime, G.W. (1994). Increased iron in the substantia nigra compacta of the MPTP-lesioned hemiparkinsonian African green monkey: evidence from proton microprobe elemental microanalysis. J. Neurochem. *62*, 134–146.

Truffi, M., Fiandra, L., Sorrentino, L., Monieri, M., Corsi, F., and Mazzucchelli, S. (2016). Ferritin nanocages: a biological platform for drug

delivery, imaging and theranostics in cancer. Pharmacol. Res. *107*, 57–65.

Vallerga, C.L., Zhang, F., Fowdar, J., Mcrae, A.F., Qi, T., Nabais, M.F., Zhang, Q., Kassam, I., Henders, A.K., Wallace, L., et al. (2020). Analysis of DNA methylation associates the cystine-glutamate antiporter SLC7A11 with risk of Parkinson's disease. Nat. Commun. *11*, 1238.

Wang, J., and Pantopoulos, K. (2011). Regulation of cellular iron metabolism. Biochem. J. *434*, 365–381.

Weinreb, O., Mandel, S., Youdim, M.B.H., and Amit, T. (2013). Targeting dysregulation of brain iron homeostasis in Parkinson's disease by iron chelators. Free Radic. Biol. Med. *62*, 52–64.

Wypijewska, A., Galazka-Friedman, J., Bauminger, E.R., Wszolek, Z.K., Schweitzer, K.J., Dickson, D.W., Jaklewicz, A., Elbaum, D., and Friedman, A. (2010). Iron and reactive oxygen species activity in parkinsonian substantia nigra. Parkinsonism Relat. Disord. *16*, 329–333.

Yang, W.S., Sriramaratnam, R., Welsch, M.E., Shimada, K., Skouta, R., Viswanathan, V.S., Cheah, J.H., Clemons, P.A., Shamji, A.F., Clish, C.B., et al. (2014). Regulation of ferroptotic cancer cell death by GPX4. Cell *156*, 317–331.

Zecca, L., Gallorini, M., Schünemann, V., Trautwein, A.X., Gerlach, M., Riederer, P., Vezzoni, P., and Tampellini, D. (2001). Iron, neuromelanin and ferritin content in the substantia nigra of normal subjects at different ages: consequences for iron storage and neurodegenerative processes. J. Neurochem. *76*, 1766–1773.

Zecca, L., Stroppolo, A., Gatti, A., Tampellini, D., Toscani, M., Gallorini, M., Giaveri, G., Arosio, P., Santambrogio, P., Fariello, R.G., et al. (2004). The role of iron and copper molecules in the neuronal vulnerability of locus coeruleus and substantia nigra during aging. Proc. Natl. Acad. Sci. U S A *101*, 9843–9848.

Zhang, S., Wang, J., Song, N., Xie, J., and Jiang, H. (2009). Up-regulation of divalent metal transporter 1 is involved in 1-methyl-4-phenylpyridinium (MPP(+))-induced apoptosis in MES23.5 cells. Neurobiol. Aging *30*, 1466–1476.

Ziering, A., and Lee, J. (1947). Piperidine derivatives; 1,3-dialkyl-4-aryl-4-acyloxypiperidines. J. Org. Chem. *12*, 911–914.

iScience, Volume *24*

Supplemental information

Apoferritin improves motor deficits in MPTP-treated mice by regulating brain iron metabolism and ferroptosis

Li-Mei Song, Zhi-Xin Xiao, Na Zhang, Xiao-Qi Yu, Wei Cui, Jun-Xia Xie, and Hua-Min Xu

Supplemental figures and legends

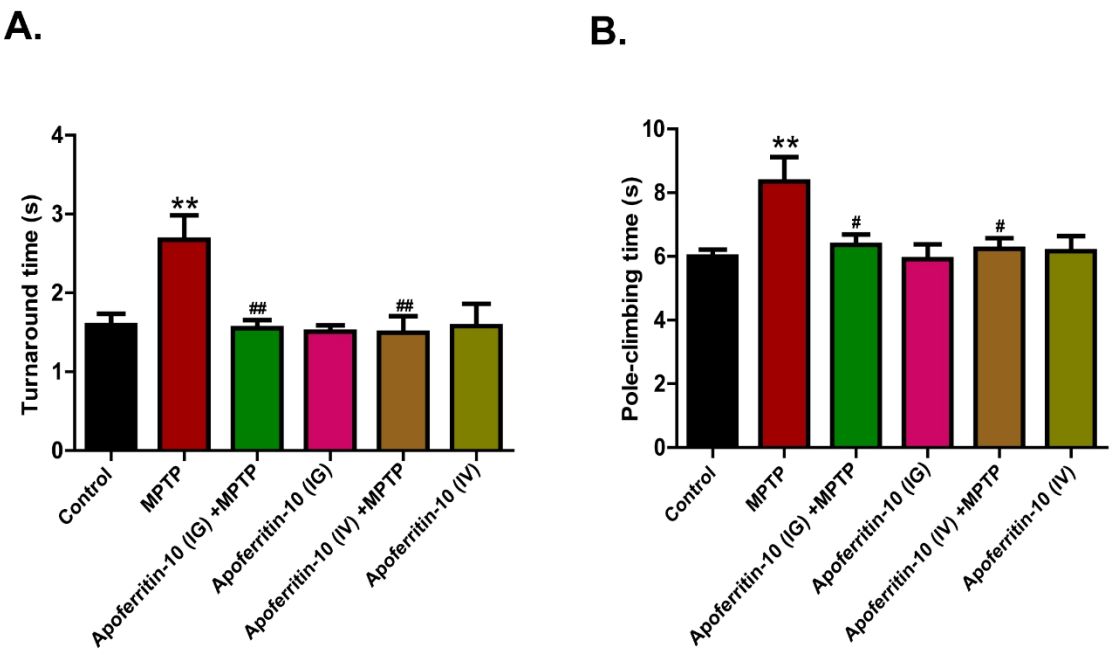

Supplementary Figure 1. Intragastric Gavage or Intravenous Injection of Apoferritin Improved Motor Deficits of MPTP-treated Mice, Related to Figure 1

MPTP resulted in significant motor deficits, which were inhibited by apoferritin given by intragastric gavage (IG) or intravenous (IV) injection. A. Turnaround time; B. Pole-climbing time. $^{**}P < 0.01$, compared with the control; $^{\#}P < 0.05$, $^{\#\#}P < 0.01$, compared with the MPTP. Data were expressed as mean ± SEM (n = 5–11 in each group).

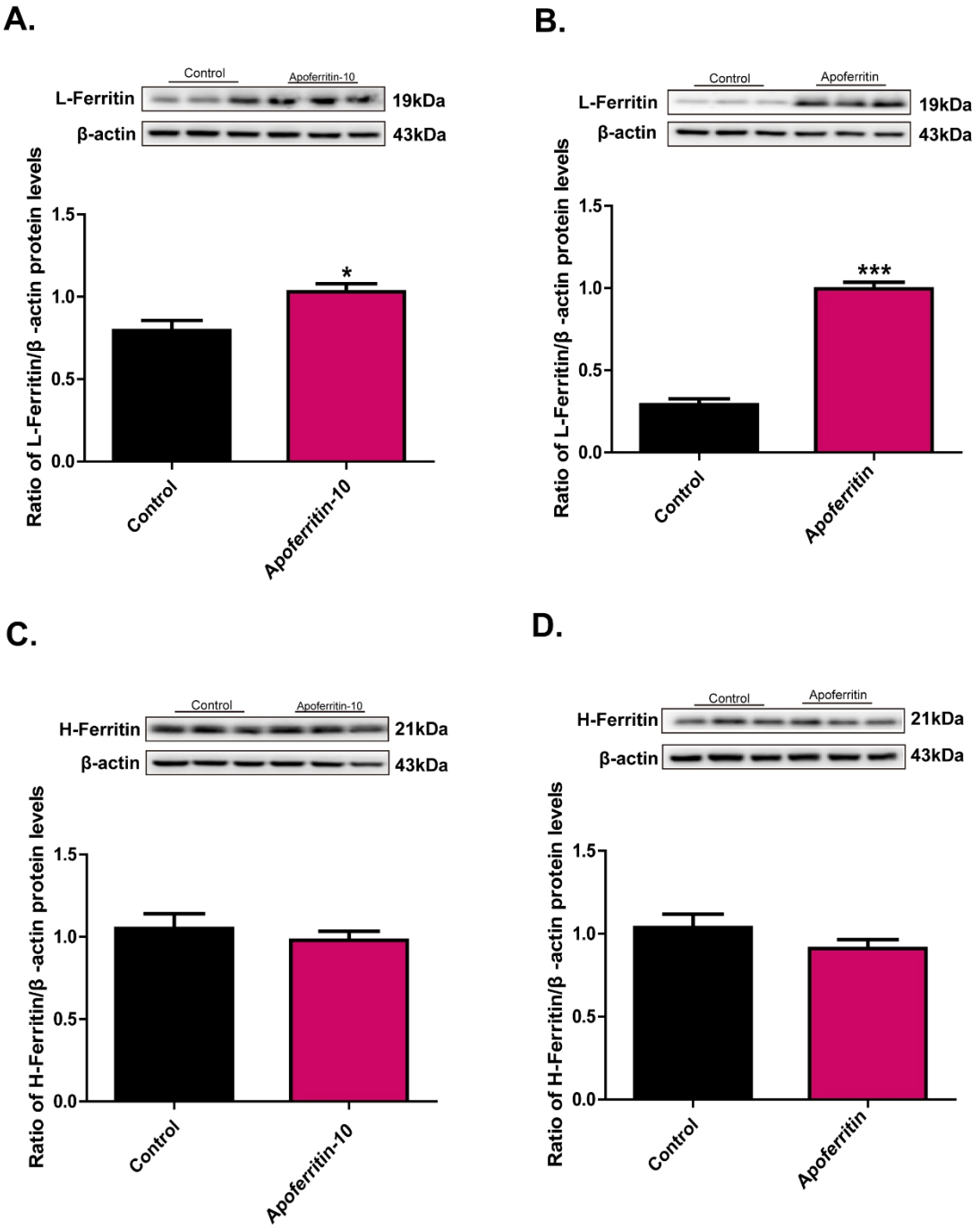

Supplementary Figure 2. The Expression of Ferritin after Apoferritin Treatment in vivo and in vitro, Related to Figure 4

The expression of L-ferritin increased significantly after apoferritin treatment, compared with the control.

A. The expression of L-ferritin in C57BL/6J mice treated with 10 mg/kg apoferritin;

B. The expression of L-ferritin in the primary VM neurons treated with 50 ug/mL apoferritin;

C. The expression of H-ferritin in C57BL/6J mice treated with 10 mg/kg apoferritin;

D. The expression of H-ferritin in the primary VM neurons treated with 50 ug/mL apoferritin.

$^{*}P < 0.05$, $^{***}P < 0.001$, compared with the control. Data was expressed as mean ± SEM (n = 6–12 in each group).

Supplementary Table 1. Key Antibodies Used in the Experiments, Related to Figure 2-5

REAGENT	WORKING DILUTION	SOURCE	IDENTIFIER
TH	1:3000/1:1000	United States Millipore	Cat# AB152; RRID: AB_390204
GPX4	1:10000	United States Abcam	Cat# ab125066; RRID: AB_10973901
FSP1	1:1000	United States Millipore	Cat# 07-2274; RRID: AB_10807552
ACSL4	1:1000	United States Santa Cruz	Cat# sc-365230; RRID: AB_10843105
β-actin	1:10000	China Bioss	Cat#bs0061R; RRID: AB_0855480
DMT1	1:1000	United States OriGene	Cat# TA324527; RRID: AB_2758340
TfR1	1:1000	United States Abcam	Cat#ab84036; RRID: AB_10673794
Iba-1	1:200	United States CST	Cat# 17198; RRID: AB_2820254
H-ferritin	1:1000	United States Abcam	Cat#ab183781
L-ferritin	1:1000	United States Abcam	Cat#ab69090; RRID: AB_1523609
Goat Anti-Rabbit IgG-Alexa Fluor 488	1:500	China Absin	Cat#abs20025
Goat Anti-Rabbit IgG-Alexa Fluor 594	1:500	China Absin	Cat#abs20021
Goat Anti-Rabbit IgG	1:10000	China Absin	Cat#abs20011
Goat Anti-Mouse IgG	1:10000	China Absin	Cat#abs20012

Transparent Methods

Method details

Chemicals

Apoferritin from horse spleen, MPTP and tyrosine hydroxylase (TH) were purchased from Sigma (St. Louis, MO, USA). The primary antibodies of glutathione peroxidase 4 (GPX4), transferrin receptor 1 (TfR1), H-ferritin and L-ferritin were from Abcam (Cambridge, MA, USA). The primary antibody of ferroptosis suppressor protein 1 (FSP1) was from MilliporeSigma (Billerica, MA, USA). The primary antibody of long-chain acyl-CoA synthetase 4 (ACSL4) was from Santa Cruz Biotechnology (CA, USA). The primary antibody of DMT1 was from OriGene Technology (Maryland, USA). The monoclonal β-actin antibody was from Bioss (Beijing, China). The goat anti-rabbit IgG labeled with HRP and goat anti-mouse IgG labeled with HRP were from absin (Shanghai, China). ECL ultrasensitive chemiluminescence kit was from MilliporeSigma (Billerica, MA, USA). Other biological reagents and materials are from local commercial sources.

Primary Cultured Ventral Mesencephalon (VM) Neurons

Primary cultures of VM neurons were obtained from embryonic 14-day Sprague–Dawley rat. Briefly, VM was dissected from the embryonic rat brain under the dissection microscope and then mechanically dissociated with a pipette until the tissue was dispersed. After centrifugation, cells were suspended in DMEM/F12 supplemented with 10% fetal bovine serum (FBS), 100 U/mL penicillin, and 100 μg/mL streptomycin and seeded on poly-d-lysine-coated 12-well culture plates. Cells were grown in a humidified atmosphere of 5% CO_2 at 37°C for 18 h, and then the culture medium was changed to serum free DMEM/F12 supplemented with 2% B27. Cells were grown for a further 4 days before use. For experiments, VM neurons were treated with 50 μg/ml Apoferritin for 24 h.

Animal Treatments

The C57BL/6J male mice used in this study were all from Vital River Laboratory Animal Technology Co. Ltd. (Beijing, China). The mice were housed one animal per cage with food pellets and water available ad libitum. The room was maintained at a constant temperature and humidity on a 12 h light/dark cycle. The mice were adapted to the laboratory environment for 1 week before the experiments. The Animal Ethics and Experimentation Committee of the Qingdao University approved the use of animals for this study.

MPTP is diluted with normal saline (NS) to 6 mg/ml, and the injection volume is 30 mg/kg; Apoferritin is diluted with NS to 2 mg/ml stock solution. The working concentration is 10 mg/kg or 15 mg/kg. Male C57BL/6J mice aged 9-10 weeks were randomly divided into four groups: control group (normal saline group), MPTP group, apoferritin+MPTP group, and apoferritin group. Pre-protection was given for 3 days before the experiments (Mice in the control group and MPTP group were given NS by intragastric gavage; Mice in apoferritin+MPTP group and apoferritin group were given apoferritin by intragastric gavage (IG) or intravenous (IV)

injection). On the 4th day after apoferritin treatment, MPTP was given intraperitoneally for 5 consecutive days to induce PD models (control group and apoferritin group intraperitoneally injected NS；MPTP group and apoferritin+MPTP group intraperitoneally injected MPTP).

Open-field Test

The open-field test was used to assess the general behavior and locomotor activity. Mice were gently placed in the center of a dedicated black box (40 cm×40 cm×40 cm). Locomotor behavior was video-recorded for 10 min by a computer for automatic analysis and the total movement distance of each animal was recorded.

Pole-climbing Test

A self-made straight wooden pole with a diameter of 1.2 cm and a height of 50 cm was used to do the pole-climbing test. A small wooden ball is placed on the top of the pole and wrapped with gauze to prevent mice from slipping. Mice were habituated to the pole on the day before testing. And then the animals were recorded via digital video on the next day. The amounts of time for the mouse to turn towards the ground (time to orient down) and to reach the ground (time to descend) were recorded. The average scores for each mouse were determined based on five tests.

Perls' Iron Staining

After the mice were perfused with NS and 4% paraformaldehyde (PFA). The brains were taken and fixed in 4% PFA for 4-6 hours, and then immersed in 20% and 30% sucrose for sugar precipitation. Brain blocks containing the SN were sectioned coronally at 20 μm on a freezing microtome and stored at -20℃. Perls' staining was utilized to detect the presence of iron in brain sections by a complex hydrated ferric ferrocyanide substance as described previously (Jiang et al., 2010). Sections were fixed with 4% PFA for 5 minutes and washed with ddH_2O for 30 seconds (not overtime). Sections were immersed for in a ready-to-use iron staining solution (2% HCL-potassium ferrocyanide), followed by three washes with PBS. Negative control sections were prepared in which the HCl and potassium ferrocyanide solutions were omitted. The sections were then immersed in 99% methanol and 1% hydrogen peroxide for 20 min to eliminate endogenous peroxidase activity. The DAB reaction product was observed under an Olympus microscope and the images were captured by a video camera (OLYMPUS, Japan) at a final magnification of 200×.

Immunofluorescence

For immunofluorescence, the sections of SN were stained with TH antibody. After three washes with 0.01% phosphate-buffered saline (PBS, pH 7.4) for 10 min, sections were incubated in 5% donkey serum-PBS for 1 h at room temperature and then incubated overnight with the primary antibody of TH (1:1000) or Iba-1(1:200). After washing, secondary antibody of Alexa Fluor ® 488 donkey anti-rabbit IgG was applied to sections for 2 h at room temperature.

Nuclei were stained with DAPI at room temperature for 10 min in the dark and washed twice with PBS. Then sections were mounted with 70% glycerin and examined using digital pathology section system (OLYMPUS, Japan). The same anatomical landmarks were used to select three sections through the SN from each mouse to count TH-positive cells at a final magnification of 400×. Values represent the mean TH-positive cells from each section.

Western Blotting

SN tissues were dissected from the brain of mice and lysed with lysis buffer on ice for 30 min. The harvested lysates were centrifuged at 12,000×g for 20 min at 4 °C, and the supernatants were used for analysis. Protein concentration was determined by a BCA protein assay kit (CWBIO China). Proteins with 5 × loading buffer (Beyotime) were incubated at 100°C for 5 min. The total 20 μg protein was separated by 8-12% SDS polyacrylamide gels and the protein in the gel was transferred to a PVDF membrane (Millipore, MA, USA). After overnight blocking with TBST containing 5% non-fat milk or BSA for 2 hours at room temperature, membranes were incubated overnight at 4 °C with the primary antibodies against TH (1:3000), DMT1 (1:800), TfR1 (1:1000), H-ferritin (1:1000), L-ferritin (1:1000), ACSL4 (1:1000), GPX4 (1:10000), FSP1 (1:1000), β-actin (1:10000). Goat anti-rabbit or goat anti-mouse IgG labeled with HRP (Santa Cruz Biotechnology, Texas, USA) was used at 1:10,000 and incubated with the membranes for 1 h at room temperature. Cross-reactivity was visualized using ECL western blotting detection reagents (Millipore, USA) and then was analyzed through scanning densitometry by a UVP BioDoc-It Imaging System (UVP, Upland, USA).

GSH/GSSG Ratio Detection

The total reduced GSH and GSSG level were detected by GSH/GSSG assay kit (Abcam, USA) according to the manufacturer's instructions. 400 μl 0.5% NP-40 (Solarbio, China) was added to 20 mg tissue to grind the tissue thoroughly, and centrifuged at 4°C, 12000 rpm for 15 min. Extract the supernatant into a new Ep tube, then add 1 volume of TCA (Abcam, USA) to 5 volume of the sample and vortex to mix. After incubation on ice for 5-10 min and centrifugation at 4°C, 12000 g for 5 min. The supernatant was used to detect the level of GSH/GSSG by GSH/GSSG assay kit. The signal was read by a fluorescence microplate reader at Ex/Em = 490/520 nm.

Statistical Analysis

The results were analyzed by GraphPad Prism 6.0 statistical software and data was expressed as mean ± SEM. One-way analysis of variance (ANOVA) followed by Turkey's test was used to compare the differences between means. $P<0.05$ was considered to be statistically significant.

Supplemental References

JIANG, H., SONG, N., XU, H., ZHANG, S., WANG, J. & XIE, J. 2010. Up-regulation of divalent

metal transporter 1 in 6-hydroxydopamine intoxication is IRE/IRP dependent. Cell Res, 20, 345-56.